


# Numerical Modeling and Optimization of Mechanical Properties in Porous Aluminum Matrix Composites Reinforced with SiC Particles

K. Mansouri<sup>a,b</sup>, S. Touati<sup>a</sup>, H. Boumediri<sup>c,\*</sup> , H. Djebaili<sup>a,b</sup>, M. Chitour<sup>a</sup>, A. Zemmouri<sup>d</sup>,  
F. Khadraoui<sup>a</sup>, A. Berkia<sup>a</sup>

<sup>a</sup>University Abbes Laghrou, Mechanical Engineering Department, 40000, Khenchela, Algeria.

<sup>b</sup>Engineering and Sciences of Advanced Materials Laboratory (ISMA), 40000, Khenchela, Algeria.

<sup>c</sup>University Frères Mentouri Constantine1, Institute of Applied Science and Technology, Algeria.

<sup>d</sup>Mechanical Engineering Department Badji Mokhtar Annaba University, Mechanics of Materials and Plant Maintenance Research Laboratory (LR3MI), Algeria.

Received: October 19, 2024; Revised: December 14, 2024; Accepted: December 30, 2024

This study investigates the impact of porosity on the mechanical properties of aluminum matrix composites reinforced with ceramic particles, focusing on the optimization of volume fraction and porosity to enhance tensile strength. Using Finite Element Analysis (FEA) and Analysis of Variance (ANOVA), the effects of varying volume fractions (5%, 10%, 15%, 20%, and 25%) and porosity levels (1%, 2%, 3%, 4%, and 5%) on Von Mises stresses were systematically analyzed. The results demonstrated that as porosity increased, Von Mises stress also increased, while higher volume fractions contributed to better stress distribution and enhanced mechanical properties. Optimization analysis identified the optimal parameters as a volume fraction of 25%, porosity level of 1.01%, particle size of 30.083  $\mu\text{m}$ , and pore diameter of 9.020  $\mu\text{m}$ , achieving a desirability score of 0.895 and a Von Mises stress of  $9.06\text{E-}08 \text{ N}/\mu\text{m}^2$ . The ANOVA results confirmed the statistical significance of these parameters, with a P-value threshold of  $<0.05$ . These insights are crucial for understanding how to optimize porosity and reinforcement in composite materials, providing valuable guidance for applications in the aerospace and automotive industries, where lightweight and high-strength materials are vital.

**Keywords:** *SiC/Al Composite, Simulation, Porosity, ANOVA, Optimization.*

## 1. Introduction

The evolution of materials has progressed from non-reinforced substances to advanced composite materials that are widely used across various industries today, particularly in automotive and aerospace applications, where lightweight materials with enhanced resistance are essential<sup>1-3</sup>. Traditional monolithic materials often fall short of these critical requirements, spurring the growing interest in material composites, which have become increasingly important due to the rising demand for high-quality engineering materials. Among these, metal matrix composites (MMCs) reinforced with ceramic particles have gained significant attention<sup>4</sup>.

Ceramic particles used in these composites can be oxides, carbides, or nitrides, and their successful application depends on specific properties such as chemical and thermodynamic stability, low diffusivity in the matrix, high interfacial energy, and isotropic behavior<sup>5,6</sup>. The inclusion of rigid reinforcing particles in a metal matrix imparts additional mechanical properties, such as high stiffness, wear resistance, low density, and a reduced thermal expansion coefficient<sup>7,8</sup>. These properties are largely determined by the type and proportion

of the reinforcing particles, the matrix material, and the interface between them. Additionally, factors such as the morphology, size, and distribution of particles significantly influence the micro-stress distribution in the material<sup>9,10</sup>.

Mechanical properties of composites are typically studied through experimental, analytical, and simulation approaches, with experimental methods being the most direct way to validate composite behavior<sup>11</sup>. However, simulations, such as finite element analysis (FEA), offer valuable insights by constructing models that replicate real-world systems while simplifying complexity. These models enable researchers to explore hypothetical scenarios that would be difficult to investigate experimentally<sup>12</sup>.

One critical factor influencing the strength of composites is porosity. The presence of pores not only reduces wettability but also weakens the bond between the matrix and the reinforcing particles, leading to diminished overall strength<sup>13,14</sup>. Numerous studies have investigated the impact of porosity in different structures. For instance, Gao et al.<sup>11</sup> developed geometric models to examine particle shapes and Representative Volume Elements (RVE) sizes in SiC/Al composites, highlighting the role of porosity in material performance.

\*e-mail: [haithem.boumediri@umc.edu.dz](mailto:haithem.boumediri@umc.edu.dz)

Christian et al.<sup>15</sup> identified surface discontinuities, such as porosity, as key factors in the initiation of fatigue cracks in stressed areas, often leading to material failure.

Further studies, such as those by Wen et al.<sup>16</sup> have demonstrated that reducing particle size in porous ceramics leads to a shift in pore size distribution and an enhancement in strength. Similarly, Aqida et al.<sup>17</sup> found that porosity significantly reduces the mechanical properties of cast MMCs by promoting void coalescence, particle fracture, and interface failure between the matrix and the reinforcement. These effects lead to decreased ductility and reduced cross-sectional area in the material. The strength of the composite is closely linked to the bond at the interfacial boundary, as observed by Chawla<sup>18</sup>, where direct contact between matrix and reinforcement atoms is necessary for strong bonding. Moreover, Zarubin and Sergeeva<sup>19</sup> developed a mathematical model to predict the thermoelastic properties of porous composites, considering porosity, matrix characteristics, and the volume fraction of reinforcing inclusions. These models enable researchers to forecast composite performance based on material parameters and porosity levels.

Recent studies have explored various strategies to optimize the mechanical properties and porosity of metal matrix composites (MMCs). Mohamad et al.<sup>20</sup> utilized peanut shell ash as reinforcement in MMCs, achieving low porosity levels (0–4%) and identifying optimal reinforcement and matrix compositions through mixture design modeling. Similarly, Parveez et al.<sup>21</sup> investigated porous aluminum composites, employing powder metallurgy and space-holder methods to enhance compressive properties by optimizing parameters like sintering temperature, compaction pressure, and particle content. Their results showed minor variations of 10.5% in plateau stress and 6.6% in energy absorption, attributed to processing and compositional differences.

Further work by Parveez et al.<sup>22</sup> focused on composites reinforced with titanium-coated diamond particles, employing Taguchi experimental design to optimize processing conditions. Wang et al.<sup>23</sup> investigated porous tantalum structures, demonstrating how microstructure optimization via 3D printing improved mechanical properties and permeability, with potential applications in biomedical implants. Additionally, Wang et al.<sup>24</sup> developed a novel liquid-nitrogen cooling approach in Wire Arc Additive Manufacturing (WAAM) to refine solidification parameters, effectively reducing porosity and enhancing the mechanical performance of Al-Cu alloys.

The goal of this study is to investigate how porosity affects the mechanical properties of aluminum matrix composites that are reinforced with ceramic particles. Specifically, the researchers want to find the best way to reduce the Von Mises stresses when the composites are pulled apart. The investigation explores a range of volume fractions (5%, 10%, 15%, 20%, and 25%) and porosity levels (1%, 2%, 3%, 4%, and 5%). This study uses FEA and ANOVA to determine the best particle size and porosity for aluminum ceramic composites in order to achieve excellent mechanical properties.

## 2. Materials Properties

The material properties used to simulate the performance of SiC/Al particles composites have been summarized in

the literature<sup>25</sup>. This paper considers the main properties of the SiC/Al composite: Young modulus, Poisson ratio, and density, which can affect the Von Mises stress distribution.

### 2.1. Matrix material

Metal matrix composites (MMCs) are widely utilized in industrial contexts as the primary form of composite material<sup>26</sup>. Aluminum matrix composites (AMCs) employ pure aluminum or an alloy as the matrix and are increasingly favored in industrial applications due to their remarkable mechanical and tribological properties. The properties of aluminum alloys can be substantially customized by introducing ceramic reinforcing particles through the process of stir casting<sup>27</sup>. The ensuing factors are utilized in every calculation<sup>28</sup>: the matrix with Young's modulus  $E_m = 70 \text{ GPa}$ , Poisson ratio  $\nu_m = 0.33$ , and density  $\rho_m = 2.7 \text{ g/cc}$ .

### 2.2. Reinforcement materials

The incorporation of Silicon carbide (SiC) as a reinforcement in composite fabrication is widespread<sup>29</sup>, with an average utilization rate of around 18%. It has been widely reported that increasing the percentage of ceramic particle reinforcement in specific ratios, while ensuring a uniform distribution, can lead to enhancements in mechanical properties. The mechanical properties of SiC particles are defined by their: Young's modulus  $E_p = 485 \text{ GPa}$ , Poisson ratio  $\nu_p = 0.2$ , and density  $\rho_p = 3.2 \text{ g/cc}$ <sup>30</sup>.

## 3. Numerical Modeling

Finite Element Analysis (FEA) has become a widely used method to model the mechanical behavior of metal matrix composites, especially those composed of aluminum and silicon carbide (SiC) at varying SiC volume fractions. Computational simulations of these composites provide valuable insights into their mechanical properties and contribute to the development of recommendations for improving structural performance. By utilizing FEA in micromechanics, this study offers an alternative to traditional analytical models, enabling more accurate simulations of reinforcement particle morphology and its effect on mechanical behavior<sup>20,31</sup>.

This research focuses on the impact of circular SiC particle morphologies and void distributions on the Von Mises stress within aluminum matrix composites. The matrix is assumed to have a square shape with a side length of  $l_m = 155.425 \mu\text{m}$ , and simulations were conducted using CASTEM<sup>32</sup> finite element software. Composites consisting of nine SiC particles were modeled in three different packing arrangements: square, hexagonal, and random, as illustrated in Figure 1. These arrangements were selected to explore how varying particle distributions influence the overall mechanical behavior of the composite material. To better understand the effects of voids and particle arrangement on the composite's mechanical properties, plane strain elements were used for modeling. This approach simulates two-dimensional behavior under tensile loading, assuming deformation occurs in a single plane. It provides an efficient and accurate analysis of the composite's response while maintaining simplicity. The model assumes that the SiC particles are perfectly bonded to the matrix, ensuring no

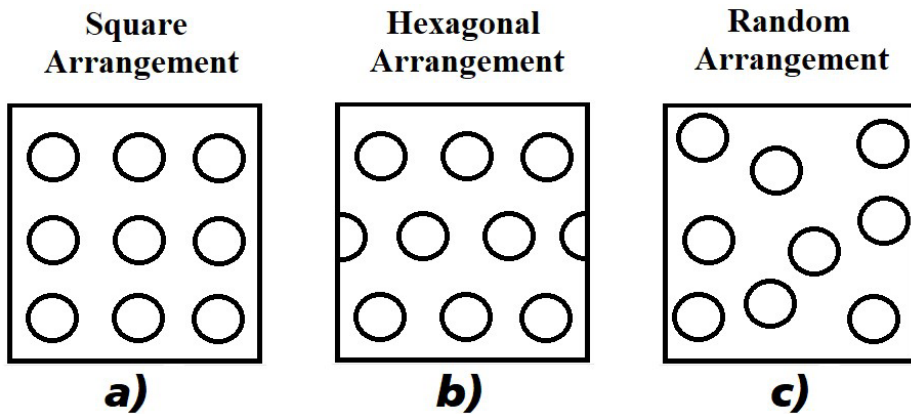


**Figure 1.** Composites with nine particles (circular form) in three different packing arrangements: a) Square, b) Hexagonal, and c) Random.

interfacial slip or debonding occurs between the particles and the matrix material. This assumption is critical for accurately modeling the ideal interaction between the reinforcing particles and the matrix. Given the small scale of the model, a refined mesh of triangular elements was employed to ensure high accuracy and convergence in the results<sup>33</sup>. This mesh refinement is essential for capturing the detailed interactions between particles, voids, and the matrix material, enabling precise prediction of stress distribution. The composite material was subjected to a uniform tensile stress ( $\sigma$ ) to simulate real-world loading conditions.

Each element in the model is assumed to have isotropic properties, meaning its material properties are uniform in all directions. For simplicity, it is assumed that all particles have an identical diameter ( $d_p$ ), reducing computational complexity while still providing meaningful insights into the composite's behavior. The specimen is modeled as a two-dimensional elastic body, with axial symmetry assumed for modeling purposes. This symmetry simplifies the analysis but still captures the key mechanical responses of the composite under loading. A periodic spatial distribution is assumed for the particles and voids, meaning the arrangement of particles and voids repeats regularly across the composite. Both the Finite Element Method (FEM) and analytical approaches rely on the assumption that voids are of identical size and shape, which simplifies calculations and comparisons<sup>34</sup>. For the purposes of this study, the composite is modeled to contain four circular voids (as shown in Figure 2), distributed according to the three arrangements (square, hexagonal, and random). These assumptions allow for a clearer understanding of the combined effects of particle arrangement and void distribution on the composite's mechanical performance.

### 3.1. Boundary conditions

The boundary conditions that characterize the application of tensile stresses to the particulate composite system, i.e., for  $x = 0$  and  $x = l_m$ ,  $U_y = 0$ , there is no motion in the y-direction for both the matrix and particles. In this case, the x-axis aligns with the length direction, and the model demonstrates axisymmetry relative to it. At the end faces of the matrix<sup>33</sup>, we exerted a force of  $F_x = 5.65 \times 10^{-8} \text{ N}/\mu\text{m}^2$ , i.e., for  $x = 0$  and  $x = l_m$  (Figure 3).

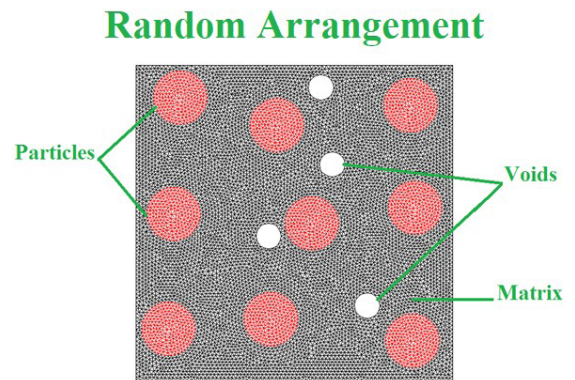


**Figure 2.** Meshed model with nine particles and four voids for random distribution.

## 4. Experimental Design and Methodology for Optimization

For this study, the experiments will use a full design matrix approach within the Response Surface Methodology (RSM) framework to find the best mechanical properties of aluminum matrix composites that are strengthened with ceramic particles. By employing a full design matrix, all possible combinations of the independent variables—volume fractions, porosity, particle size, and pore diameter—will be systematically explored. This thorough approach ensures that the study captures the complete interaction effects between these variables, providing a robust dataset for analysis. After the data is gathered, polynomial regression will be used to make a model of the response surface. This model will show how the input factors relate to Von Mises stresses<sup>35</sup>. To assess the model's significance and the influence of individual factors, an Analysis of Variance (ANOVA) will be performed. Von Mises stresses that ANOVA will play a critical role in identifying which factors and interactions significantly impact the response variable. This statistical analysis will allow for a deeper understanding of the relationships within the model, guiding the refinement of the polynomial regression to include only the most impactful terms. This process will ensure that

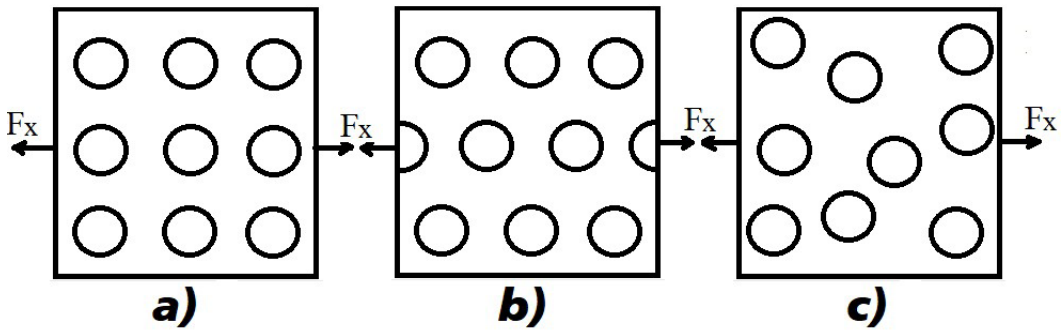


**Figure 3.** Boundary conditions for three packing: a) square, b) hexagonal and c) random

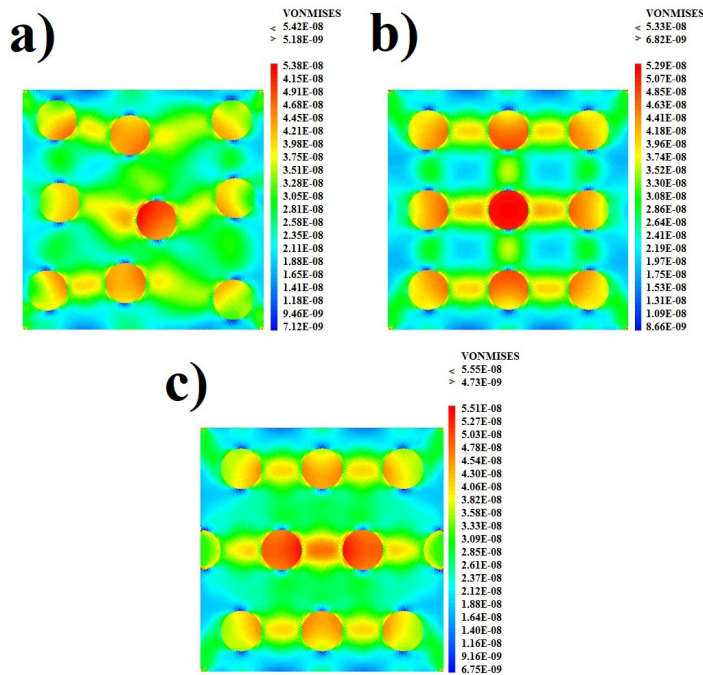


**Figure 4.** Von Mises Stress distributions for  $V_f = 20\%$  for: a) square, b) hexagonal and c) random

the resulting model is both accurate and efficient, laying the groundwork for effective optimization<sup>36</sup>. The desirability function will be employed for the optimization phase, a method commonly used in multi-response optimization. The desirability function will transform each response into a value between 0 (undesirable) and 1 (desirable), and the overall desirability will be computed as the geometric mean of these individual values. This approach will enable the simultaneous optimization of multiple responses, allowing the study to identify the optimal combination of input variables that will achieve the desired mechanical properties<sup>37</sup>.

## 5. Results and Discussions

### 5.1. Composite without porosity

This section discusses the results of the simulation. Von Mises stress distributions on the composites with no

defects and no pores in the three packing are shown in Figure 4. We can find the following: the stresses are concentrated in the SiC reinforcements and in the areas between these particles; the different deformations in different parts of the matrix resulted in additional stress and generated non-uniform stress distribution.

As shown in Figure 5, the Von Mises stresses decrease as the volume fraction of the reinforcement material increases across all three arrangement types, up to a volume fraction ( $V_f$ ) of 30%. Beyond this point, the stresses stabilize and then begin to increase in both the hexagonal and square arrangements. These ideal packing arrangements are often used in micromechanical models due to their simplicity; however, they are rarely observed in real composites except in localized regions. In contrast, the random arrangement, which is more representative of real composites, shows a sudden increase in Von Mises stresses. This is due to the



closer proximity of particles in random arrangements, which results in localized concentrations of additional stresses.

## 5.2. Composite with porosity

In the following section, we introduce voids into the previously studied composite (Figure 6), distributing four pores across the three packing arrangements. The porosity ranged from 1% to 5%, as composites with porosity levels above 5% were considered unsuitable.

The stresses are always concentrated in the SiC particles and in the areas between these reinforcements, as shown in Figure 7. Porosity has a significant impact on the distribution of stress within a matrix material. When voids are present in the matrix, the stress in these regions is relatively low along the tensile direction, while higher stresses are observed on either side of the voids. This uneven stress distribution is due to the presence of pores within the composite material. In the composite without voids, it is noted that when the volume fraction of the particles increases, the Von Mises stresses decrease, and this is true for the three types of distribution up to 30%.

In the composite with porosity, it is noted that when porosity increases, the stresses also increase (Figure 8). In the random distribution (Figure 8c), we can see that the stresses have large values compared to the square and hexagonal; this is due to the presence of voids between the particles, which in turn increases the stress concentrations.

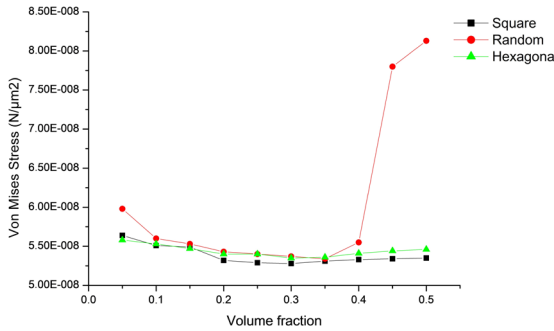


**Figure 5.** Evolution of Von Mises stresses in function of volume fraction.

## 5.3. Optimization of Von Mises stresses

Table 1 presents data generated to optimize the mechanical properties of Aluminum matrix composites reinforced with ceramic particles. The study investigates the effects of varying volume fractions (0.05% to 0.25%) and porosity levels (0.1% to 0.5%) on particle size, pore diameter, and Von Mises stresses. As porosity increases within each volume fraction, pore diameter also increases, which is consistent across all simulations. The particle size remains constant for each volume fraction but differs between them, ranging from 13.46  $\mu\text{m}$  at 0.05% volume fraction to 30.09  $\mu\text{m}$  at 0.25%. Von Mises stresses, indicative of the material's yield strength under tensile load, generally increase with higher volume fractions and porosity levels. The analysis indicates that lower volume fractions and porosity levels tend to exhibit lower Von Mises stresses, suggesting higher strength and durability under tensile loading. Conversely, higher volume fractions and porosity levels lead to increased pore diameters and variations in Von Mises stresses, potentially affecting composite performance. The data highlight the significant impact of these parameters on the mechanical properties of the composites, providing a foundation for optimizing material performance through the Taguchi Method. This structured approach systematically explores the effects of multiple variables, aiding in identifying optimal conditions for enhanced composite material properties.

### 5.3.1. ANOVA for quadratic model of Von Mises stresses

Table 2 summarizes the Analysis of Variance (ANOVA) results for the optimization model employed in this study. It presents the sources of variation, sum of squares, degrees of freedom (DF), mean square, F-value, P-value, and significance remarks for each factor analyzed. The ANOVA results reveal that the overall model is statistically significant, with a P-value of less than 0.0001, indicating that the model adequately explains the variation in the data. A P-value threshold of  $<0.05$  was applied to assess statistical significance for individual factors and their interactions, confirming the relevance of the factors considered in the model<sup>38-41</sup>. While individual factors such as volume fraction (A), porosity (B), particle diameter (C), and pore diameter (D) did not have significant effects on the outcome (P-values  $>0.05$ ),

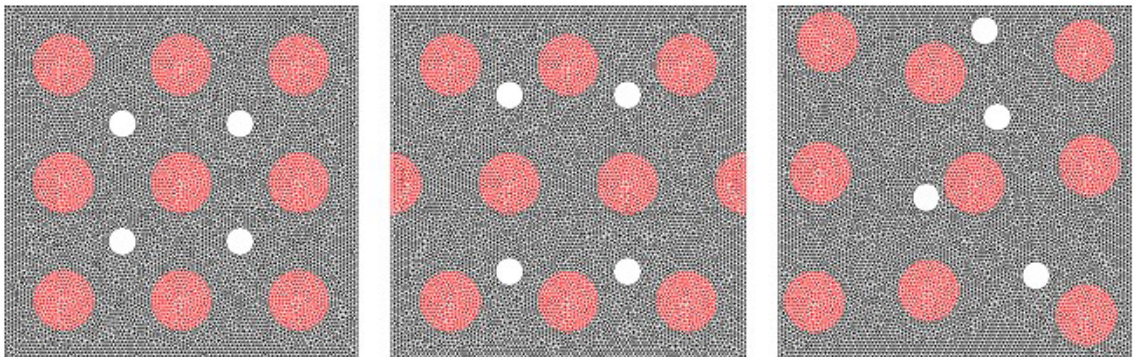


**Figure 6.** Composite model mesh with different packing.

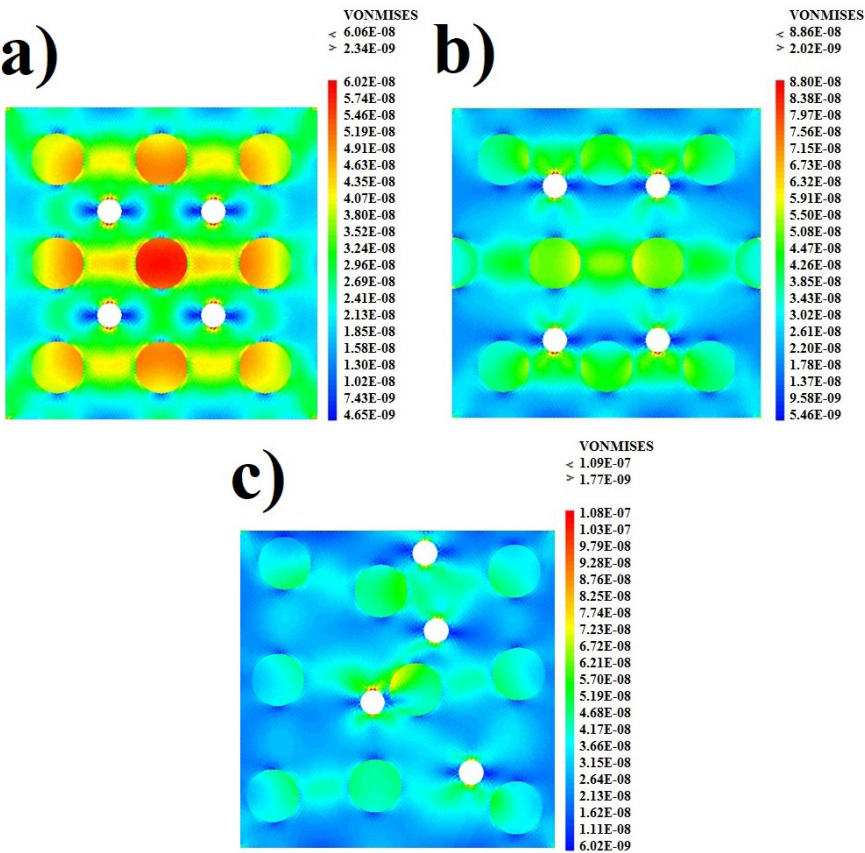


Figure 7. Von Mises stress distribution  $V_f=20\%$  of particles and for a porosity of 3% for: a) square, b) hexagonal and c) random.

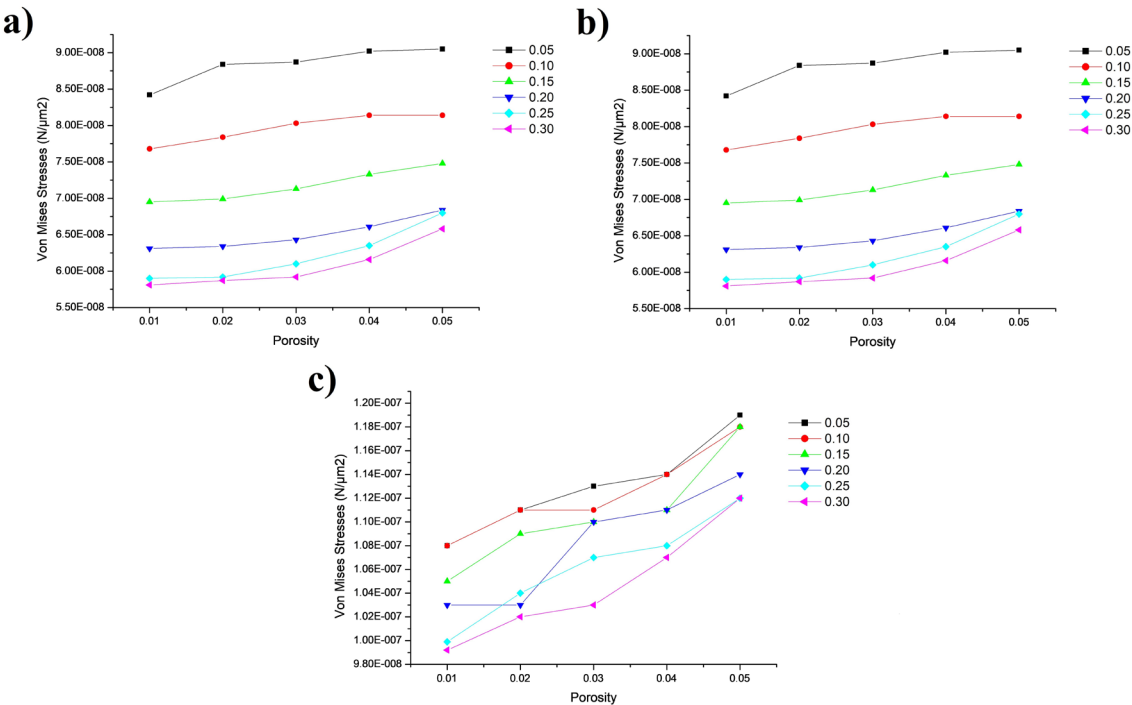


Figure 8. Evolution of Von Mises stresses in function of porosity for: a) square, b) hexagonal and c) random.

**Table 1.** Mechanical properties for aluminum matrix composites reinforced with ceramic particles.

Run	Volume Fractions (%)	Porosity (%)	Particle Size ( $\mu\text{m}$ )	Pore Diameter ( $\mu\text{m}$ )	Von Mises stresses ( $\text{N}/\mu\text{m}^2$ )
1	0.05	0.1	13.46	9.02	1.08E-07
2	0.05	0.2	13.46	12.72	1.13E-07
3	0.05	0.3	13.46	15.63	1.14E-07
4	0.05	0.4	13.46	18.05	1.15E-07
5	0.05	0.5	13.46	20.19	1.19E-07
6	0.1	0.1	19.09	9.02	1.08E-07
7	0.1	0.2	19.09	12.72	1.11E-07
8	0.1	0.3	19.09	15.63	1.11E-07
9	0.1	0.4	19.09	18.05	1.14E-07
10	0.1	0.5	19.09	20.19	1.18E-07
11	0.15	0.1	23.31	9.02	1.05E-07
12	0.15	0.2	23.31	12.72	1.09E-07
13	0.15	0.3	23.31	15.63	1.1E-07
14	0.15	0.4	23.31	18.05	1.11E-07
15	0.15	0.5	23.31	20.19	1.18E-07
16	0.2	0.1	26.92	9.02	1.03E-07
17	0.2	0.2	26.92	12.72	1.03E-07
18	0.2	0.3	26.92	15.63	1.1E-07
19	0.2	0.4	26.92	18.05	1.11E-07
20	0.2	0.5	26.92	20.19	1.14E-07
21	0.25	0.1	30.09	9.02	9.09E-08
22	0.25	0.2	30.09	12.72	1.04E-07
23	0.25	0.3	30.09	15.63	1.08E-07
24	0.25	0.4	30.09	18.05	1.07E-07
25	0.25	0.5	30.09	20.19	1.12E-07

**Table 2.** ANOVA Results for Von Mises stresses.

Source	Sum of Squares	DF	Mean Square	F-value	P-value	Remark
Model	8.135E-16	12	6.779E-17	26.34	< 0.0001	Significant
A-VOLUME	1.758E-19	1	1.758E-19	0.0683	0.7983	No-Significant
B-POROSITY	2.911E-18	1	2.911E-18	1.13	0.3085	No-Significant
C-D par	1.397E-19	1	1.397E-19	0.0543	0.8197	No-Significant
D-D por	3.005E-18	1	3.005E-18	1.17	0.3012	No-Significant
AB	2.096E-17	1	2.096E-17	8.14	0.0145	Significant
AC	1.108E-19	1	1.108E-19	0.0430	0.8391	No-Significant
AD	2.430E-17	1	2.430E-17	9.44	0.0097	Significant
BC	1.800E-17	1	1.800E-17	6.99	0.0214	Significant
BD	2.106E-18	1	2.106E-18	0.8182	0.3835	No-Significant
CD	2.052E-17	1	2.052E-17	7.97	0.0154	Significant
A <sup>2</sup>	1.953E-19	1	1.953E-19	0.0759	0.7876	No-Significant
B <sup>2</sup>	1.351E-18	1	1.351E-18	0.5250	0.4826	No-Significant
Residual	3.089E-17	12	2.574E-18			
Cor Total	8.444E-16	24				

interaction effects between factors (AB, AD, BC, and CD) demonstrated a significant influence, with P-values below 0.05. Specifically, the interactions between volume fraction and porosity (AB), volume fraction and pore diameter (AD), porosity and particle diameter (BC), and particle diameter and pore diameter (CD) were found to have a substantial impact on the mechanical properties of the aluminum matrix composites. These findings highlight the importance

of considering the combined effects of these variables in optimizing composite material properties.

### 5.3.2. Fit statistics of Von Mises stresses

Table 3 presents the fit statistics for the quadratic model used to predict Von Mises stresses in the optimization of Aluminum matrix composites. The model's standard deviation, mean response, coefficient of variation (C.V.

%), and various R<sup>2</sup> values (R<sup>2</sup>, R<sup>2</sup>-Adjusted, R<sup>2</sup>-Predicted) are displayed along with the Adequate Precision metric. A high R<sup>2</sup> value of 0.9634 suggests the model fits the data well. The R<sup>2</sup>-Adjusted and R<sup>2</sup>-Predicted values are also high, further confirming the model's robustness and reliability. Adequate Precision, which measures the signal-to-noise ratio, is 23.0139, indicating a very strong signal, well above the threshold value of 4, suggesting the model can effectively explore the design space.

The equation for predicting “Von Mises” is as follows:

Von Mises stresses = -- 2.9190 · x · 10<sup>-7</sup> · ... · 2.5019 · x · 10<sup>-6</sup> · x · A · -4.0186 · x · 10<sup>-6</sup> · x · B · + · 2.3428 · x · 10<sup>-8</sup> · x · C · + · 7.5741 · x · 10<sup>-8</sup> · x · D · ... · 7.1326 · x · 10<sup>-6</sup> · x · AB · + · 2.0430 · x · 10<sup>-8</sup> · x · AC · + · 2.7583 · x · 10<sup>-7</sup> · x · AD · + · 7.9902 · x · 10<sup>-8</sup> · x · BC · + 1.1594 · x · 10<sup>-7</sup> · x · BD · -3.0640 · x · 10<sup>-9</sup> · x · CD · - · 1.2159 · x · 10<sup>-6</sup> · x · A<sup>2</sup> · ... · 1.1429 · x · 10<sup>-6</sup> · x · B<sup>2</sup>q

This equation captures the influence of individual factors and their interactions on Von Mises stresses within the Aluminum matrix composites. The coefficients reflect how changes in these factors affect the stress outcomes, with interactions between variables and squared terms included to address their combined effects. The Normal Plot of Residuals in Figure 9a assesses the normality of the residuals, which are the differences between the observed and predicted Von Mises stresses. In this plot, the residuals are color-coded based on their corresponding Von Mises stress values, ranging from lower stresses (blue) to higher stresses (red). The data points closely follow the reference diagonal line, suggesting

that the residuals are approximately normally distributed. This is an important diagnostic tool, as it indicates that the regression model's assumptions, particularly the error terms' normality, are likely satisfied. Any significant deviation from this line would suggest potential issues with the model, such as non-normality of errors or the presence of outliers, but the observed alignment here supports the validity of the model.

Figure 9b show the Predicted vs. Actual Plot compares the predicted Von Mises stresses generated by the model with the actual observed stresses. Each point on the plot represents a pair of actual and predicted values, and the closer these points are to the diagonal line, the more accurate the model's predictions. The plot shows a strong alignment of the points along this line, indicating that the model has high predictive accuracy. The color gradient, which transitions from blue (representing lower Von Mises stresses) to red (higher stresses), helps visualize how well the model predicts across the spectrum of stress values.

The uniform distribution of points along the diagonal across all stress levels suggests that the model consistently predicts well without significant bias toward overestimating or underestimating the stresses. This reinforces the model's reliability for use in optimizing the mechanical properties of the composite material.

Figure 10 effectively illustrates the key interaction effects that influence the Von Mises stresses in aluminum matrix composites, which are critical for understanding the material's mechanical performance. The 3D surface plots (a) through (d) show the combined effects of different pairs of factors: Volume Fractions and Porosity, Volume Fractions and Pore Diameter, Porosity and Particle Size, and Particle Size and Pore Diameter, respectively. Each plot uses a gradient color

Table 3. Fit statistics for Quadratic Model of Von Mises Stresses.

Response	Std. dev.	Mean	C.V. %	R <sup>2</sup>	R <sup>2</sup> -Adjusted	R <sup>2</sup> -Predicted	Adeq Precision
VON mis	1.604E-09	1.099E-07	1.46	0.9634	0.9268	0.8138	23.0139

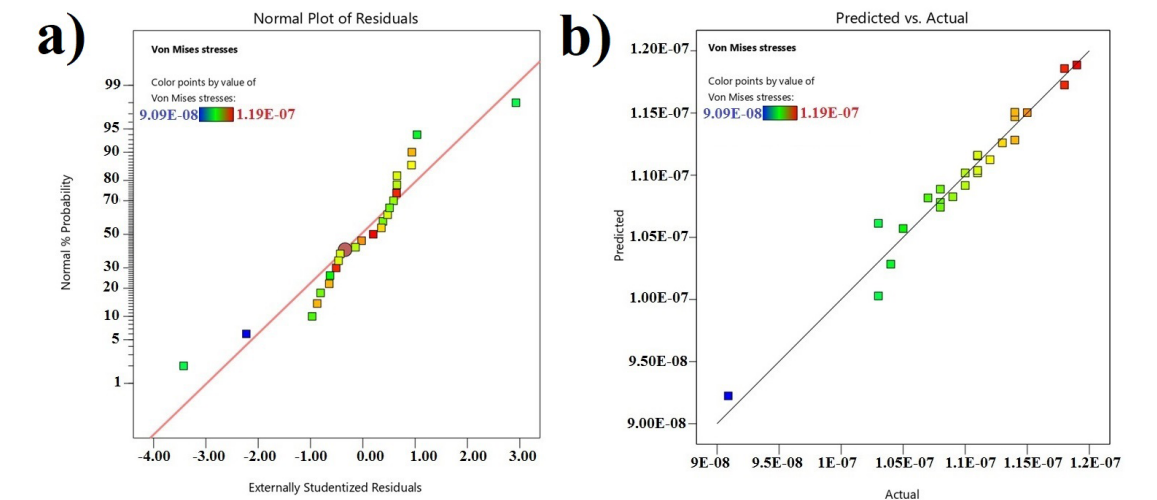
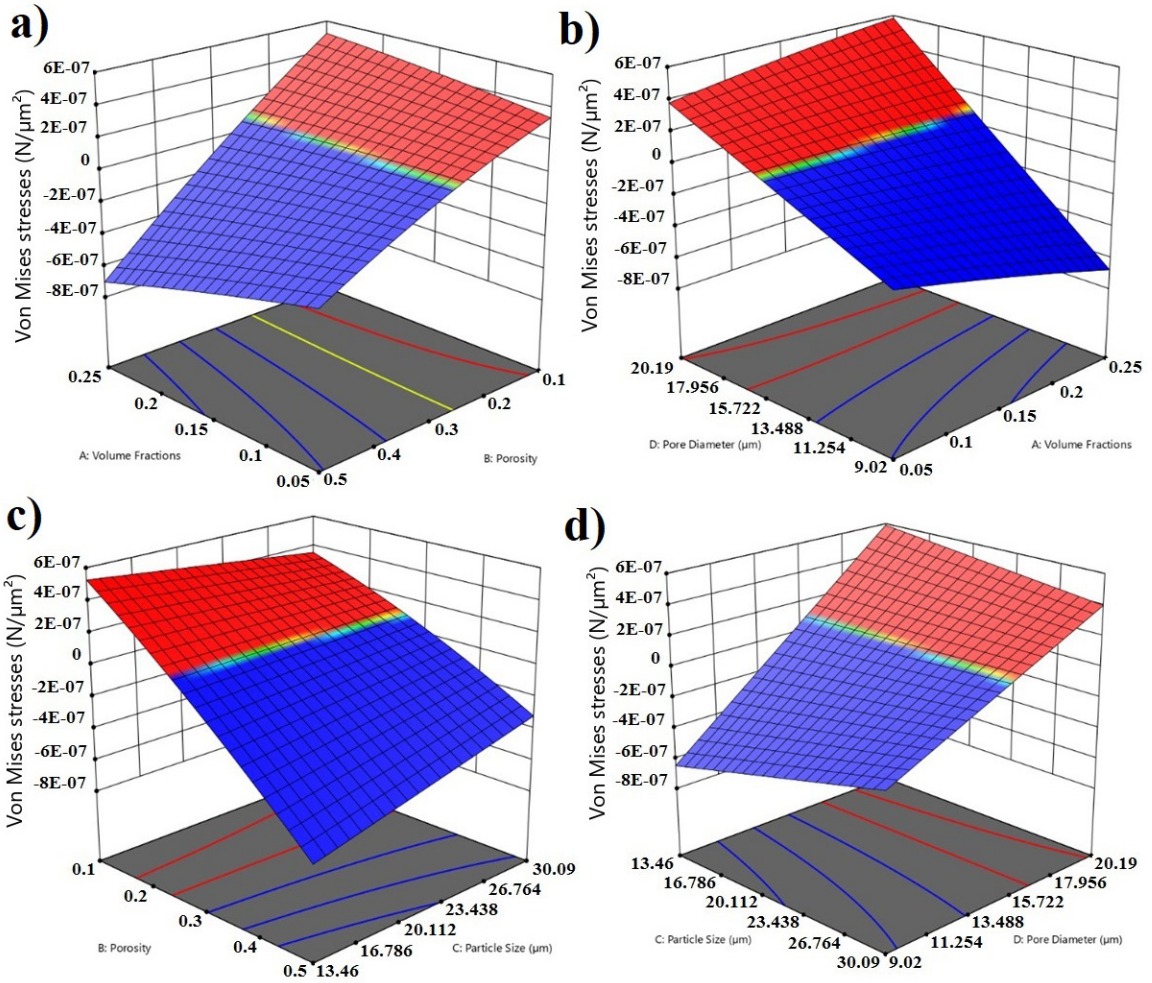


Figure 9. (a) Normal Plot of Residuals, (b) Predicted vs. Actual Plot for Von Mises Stresses in Aluminum Matrix Composites.





**Figure 10.** 3D Surface Plots of Von Mises Stresses for Aluminium Matrix Composites, Showing the Interaction Effects of (a) Volume Fractions and Porosity, (b) Volume Fractions and Pore Diameter, (c) Porosity and Particle Size, and (d) Particle Size and Pore Diameter.

scheme to represent the stress levels, where red indicates higher stresses and blue indicates lower stresses.

These visualizations reveal that the interactions between these factors are not only significant but are also the primary drivers in determining the material's yield strength under tensile load. For instance, the interaction between Volume Fractions and Porosity in the plot (a) demonstrates that as both parameters increase, the Von Mises stresses rise, suggesting a synergistic effect that reduces material strength. Similarly, the interaction between Particle Size and Pore Diameter in the plot (d) shows a similar trend; where smaller particles combined with larger pore diameters result in higher stresses. These results underscore the importance of understanding and optimizing these interactions to improve the composite material's performance. By carefully controlling these variables, engineers can better design composites that withstand higher stresses, thereby enhancing their applicability in demanding environments.

### 5.3.3. Desirability function

The optimization study identified three optimal solutions using the desirability function, which transforms multiple

response variables into a unified desirability score ranging from 0 (undesirable) to 1 (ideal)<sup>36</sup>. The overall desirability score is calculated as the geometric mean of individual desirability values, enabling the simultaneous optimization of multiple responses. This method provides a systematic approach to balance conflicting objectives, such as minimizing porosity while maximizing mechanical performance. The best solution achieved a desirability score of 0.895, corresponding to a volume fraction of 25%, porosity of 1.01%, particle size of 30.083  $\mu\text{m}$ , and pore diameter of 9.020  $\mu\text{m}$ . These parameters resulted in a Von Mises stress of 9.06E-08  $\text{N}/\mu\text{m}^2$ , reflecting an optimal balance between mechanical properties and composite structure (Table 4).

Additional solutions with slightly lower desirability scores (0.890 and 0.863) were also identified, offering alternative parameter combinations that may suit different application requirements. While the desirability function effectively optimized the composite's mechanical properties, it has certain limitations. The method's reliance on weighting factors for individual responses may introduce bias, especially if the weights are not accurately determined based on experimental or practical priorities. Furthermore, the geometric mean used

**Table 4.** Best 3 solutions found using desirability function.

Number	Volume Fractions (%)	Porosity (%)	Particle Size (μm)	Pore Diameter (μm)	Von Mises stresses (N/μm <sup>2</sup> )	Desirability
1	<b>0.250</b>	<b>0.101</b>	<b>30.083</b>	<b>9.020</b>	<b>9.06E-08</b>	<b>0.895</b>
2	0.250	0.105	30.085	9.216	9.07E-08	0.890
3	0.250	0.500	13.460	9.020	9.10E-08	0.863

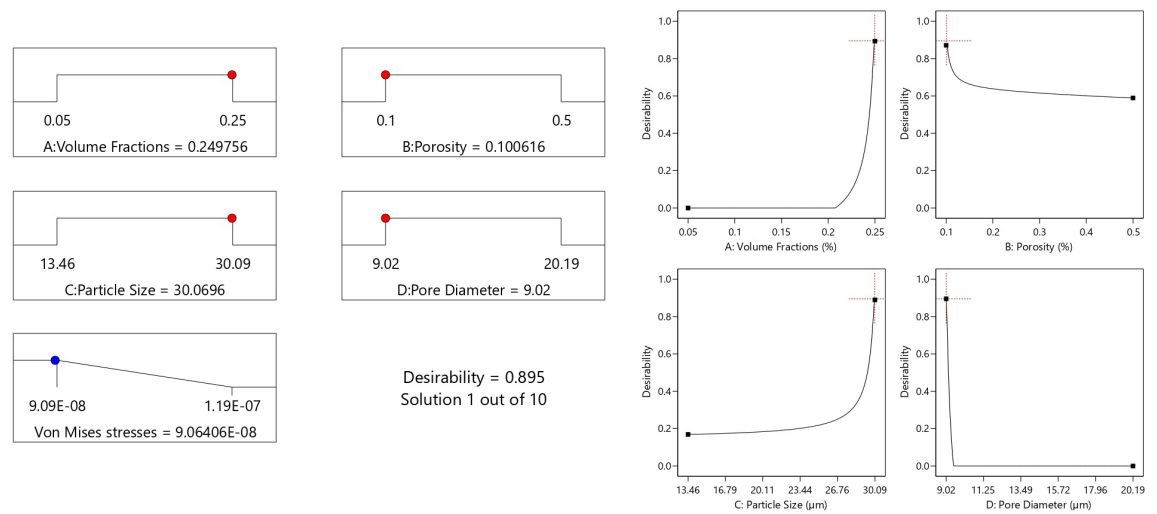


**Figure 11.** The best combinations of parameters found using desirability function.

in the calculation may overly penalize individual responses with lower desirability values, potentially skewing the optimization results.

Figure 11 further illustrates the optimization process, showing how the desirability function varies with changes in each parameter. The steep curves in the desirability plots indicate the sensitivity of the material properties to these factors, with slight adjustments leading to significant changes in the overall desirability score. This highlights the critical role that precise tuning of Volume Fractions, Porosity, Particle Size, and Pore Diameter plays in optimizing the material’s performance. The visual representation of the best solution in the first figure underscores the effectiveness of this approach, providing a clear roadmap for achieving the desired mechanical properties in aluminum matrix composites.

**6. Conclusions**

In this study, aluminum matrix composites reinforced with SiC particles were evaluated at varying volume fractions (5% to 30%) and porosity levels (0.01 to 0.05). Mechanical properties were calculated using random packing arrangements, and the key findings of the study are as follows:

- **Impact of Pores on Stress Distribution:** The presence of pores significantly affects the stress distribution within the composite matrix. Stress concentrations were observed around the voids, leading to lower stress in the matrix and resulting in substantial plastic deformation and potential failure under tensile loading. Understanding these

stress patterns is essential for designing composites with enhanced mechanical properties and better resistance to deformation.

- **Strong Predictive Reliability:** The regression model developed in this study accurately captured the relationship between input parameters—volume fractions, porosity, particle size, and pore diameter—and Von Mises stresses. With a high  $R^2$  value of 0.9634, the model demonstrated strong predictive reliability, providing a valuable tool for optimizing composite material performance.
- **Significant Interactions Identified by ANOVA:** ANOVA results revealed significant interactions between key factors, such as volume fraction and porosity (P-value = 0.0145) and particle size and pore diameter (P-value = 0.0154). These interactions play a critical role in determining the mechanical performance of the composites, highlighting the importance of considering combined effects in material design.
- **Optimization of Mechanical Properties:** The desirability function identified the optimal parameter combinations for the composite material, achieving a desirability score of 0.895. This balanced approach led to a significant enhancement in mechanical properties, confirming the effectiveness of the optimization process.
- These findings have important implications for industries like aerospace and automotive, where lightweight and high-strength materials are

critical. The optimization of porosity and particle reinforcement offers the potential for developing advanced composite materials with superior mechanical properties, providing solutions for more efficient, durable, and sustainable materials in demanding engineering applications.

## 7. References

1. Lira HMD, Barbosa WADO, Pina EACD, Moura ADAD, Rodriguez PR, Melo IRD, et al. Manufacturing of AA7075 aluminum alloy composites reinforced by nanosized particles of SiC, TiN, and ZnO by high-energy ball milling and hot extrusion. *Mater Res*. 2023;26:e20230154. <http://doi.org/10.1590/1980-5373-mr-2023-0154>.
2. Chitour M, Khadraoui F, Mansouri K, Rebai B, Menasria A, Zemmouri A, et al. A novel high order theory for static bending of functionally graded (FG) beams subjected to various mechanical loads. *Research on Engineering Structures and Materials*. 2024;10:10. <http://doi.org/10.17515/resm2024.141me0104rs>.
3. Zakeri M, Vakili-Ahrari Rudi A. Effect of shaping methods on the mechanical properties of Al-SiC composite. *Mater Res*. 2013;16(5):1169-74. <http://doi.org/10.1590/S1516-14392013005000109>.
4. Litouche B, Rebai B, Mansouri K. Investigating the impact of flow profile on heat transfer in nanofluid flow: a numerical study. *Mechanika*. 2024;30(2):177-82. <http://doi.org/10.5755/j02.mech.34638>.
5. Prasad DS, Shoba C, Ramanaiah N. Investigations on mechanical properties of aluminium hybrid composite. *J Mater Res Technol*. 2014;3(1):79-85. <http://doi.org/10.1016/j.jmrt.2013.11.002>.
6. Hemanth KTR, Swamy RP, Chandrashekar TK. Taguchi technique for the simultaneous optimization of tribological parameters in metal matrix composite. *J Miner Mater Charact Eng*. 2011;10(12):1179-88. <http://doi.org/10.4236/jmmce.2011.1012090>.
7. Dobrzański LA, Kremzer M, Nagel A, Huchler B. Composite materials based on the porous Al<sub>2</sub>O<sub>3</sub> ceramics infiltrated with the EN AC – AlSi12 alloy. *Kompozyty*. 2005;4a:35-44.
8. Cao C, Zhang X, Chen T, Chen Y. Effects of processing parameters on microstructure and mechanical properties of powder-thixoforged SiCp/6061 Al composite. *Mater Res*. 2017;20(1):236-48. <http://doi.org/10.1590/1980-5373-mr-2016-0466>.
9. Park HK, Jung J, Kim HS. Three-dimensional microstructure modeling of particulate composites using statistical synthetic structure and its thermo-mechanical finite element analysis. *Comput Mater Sci*. 2017;126:265-71. <http://doi.org/10.1016/j.commatsci.2016.09.033>.
10. Hadjez F, Maouche H, Boumediri H, Chorfi S, Boukelia TE. Se (IV)-Doped Monodisperse Spherical TiO<sub>2</sub> Nanoparticles for Adhesively Bonded Joint Reinforcing: synthesis and Characterization. *SAE Int J Mater Manuf*. 2024;17(3):233-44. <http://doi.org/10.4271/05-17-03-0017>.
11. Gao Z, Gao H, Zhang Y, Wu Q, Chen S, Zhou X. Study on stress distribution of SiC/Al composites based on microstructure models with microns and nanoparticles. *Nanotechnol Rev*. 2022;11(1):1854-69. <http://doi.org/10.1515/ntrev-2022-0112>.
12. Banks J, Carson JS II, Nelson BL, Nicol DM. Discrete: event system simulation. 5th ed. New Jersey: Pearson Education; 2010.
13. Priyadarshi D, Sharma RK. Porosity in aluminum matrix composites: cause, effect and defence. *Mater Sci Indian J*. 2016;14(4):119-29.
14. Mohammed KA, Talib RA, Algburi S, Kareem A, Bhavani B, Alkhafaji MA, et al. Synthesis PEO/PS/PMMA/Se as new nanocomposite with porous morphology. *Chalcogenide Lett*. 2023;20(12):863-70. <http://doi.org/10.15251/CL.2023.2012.863>.
15. Christian JL, Forest JD, Weisinger MD. Aluminum-boron composites for aerospace structures. San Diego: General Dynamics Corp.; 1970.
16. Wen Y, Nan L, Han BQ. High-strength, lightweight spinel refractories. *Am Ceram Soc Bull*. 2005;84(4):1-3.
17. Aqida SN, Ghazali MI, Hashim J. Effects of porosity on mechanical properties of metal matrix composite: an overview. *J Teknol*. 2004;40:17-32.
18. Chawla KK. Composite materials: science and engineering. New York: Springer Verlag; 1987. <http://doi.org/10.1007/978-1-4757-3912-1>.
19. Zarubin VS, Sergeeva ES. Effects of porosity of a composite reinforced with nanostructured inclusions on its thermoelastic characteristics. *Mech Solids*. 2018;53(6):675-84. <http://doi.org/10.3103/S0025654418060080>.
20. Refaai MRA, Reddy RM, Venugopal J, Rao MV, Vaidhegi K, Yishak S. Optimization on the mechanical properties of aluminium 8079 composite materials reinforced with PSA. *Adv Mater Sci Eng*. 2022;2022:11. <http://doi.org/10.1155/2022/6328781>.
21. Parveez B, Jamal NA, Aabid A, Baig M, Yusof F. Experimental analysis and parametric optimization on compressive properties of diamond-reinforced porous Al composites. *Materials*. 2023;16(1):91. <http://doi.org/10.3390/ma16010091>.
22. Parveez B, Jamal NA, Maleque MA, Rozhan AN, Aabid A, Baig M. Optimizing the compressive properties of porous aluminum composites by varying diamond content, space holder size and content. *Materials*. 2023;16(3):921. <http://doi.org/10.3390/ma16030921>.
23. Wang Y, Qin X, Lv N, Gao L, Sun C, Tong Z, et al. Microstructure optimization for design of porous tantalum scaffolds based on mechanical properties and permeability. *Materials*. 2023;16(24):7568. <http://doi.org/10.3390/ma16247568>.
24. Wang Z, Lu X, Lin X, Hao Z, Hu C, Feng Z, et al. Porosity control and properties improvement of Al-Cu alloys via solidification condition optimisation in wire and arc additive manufacturing. *Virtual Phys Prototyp*. 2024;19(1):e2414408. <http://doi.org/10.1080/17452759.2024.2414408>.
25. Arreola-Herrera R, Cruz-Ramírez A, Rivera-Salinas JE, Romero-Serrano JA, Sánchez-Alvarado RG. The effect of non-metallic inclusions on the mechanical properties of 32 CDV 13 steel and their mechanical stress analysis by numerical simulation. *Theor Appl Fract Mech*. 2018;94:134-46. <http://doi.org/10.1016/j.tafmec.2018.01.013>.
26. Kareem A, Qudeiri JA, Abdudeen A, Ahammed T, Ziout AA. Review on AA 6061 metal matrix composites produced by stir casting. *Materials*. 2021;14(1):1-22. <http://doi.org/10.3390/ma14010175>.
27. Muhammad F, Shawnam J. Optimization of stirrer parameters by Taguchi method for a better ceramic particle stirring performance in the production of aluminum alloy matrix composite. *Cogent Eng*. 2023;10(1):2154005. <http://doi.org/10.1080/23311916.2022.2154005>.
28. Keiichiro T, Yu I, Yoshinobu S. A constitutive model of particulate-reinforced composites taking account of particle size effects and damage evolution. *Compos, Part A Appl Sci Manuf*. 2010;41(2):313-21. <http://doi.org/10.1016/j.compositesa.2009.10.023>.
29. Kumar P, Kumar A, Kumar A, Lavkush, Kumar Y, Dwivedi SP. Different reinforcement particles and their effects in the development of composite material by different development techniques: a review. *Mater Today Proc*. 2021;47:4015-9. <http://doi.org/10.1016/j.matpr.2021.04.267>.
30. Laghari RA, Li J, Wu Y. Study of machining process of SiCp/Al particle reinforced metal matrix composite using finite element analysis and experimental verification. *Materials*. 2020;13(23):5524. <http://doi.org/10.3390/ma13235524>.
31. Rivera-Salinas JE, Gregorio-Jáuregui KM, Romero-Serrano JA, Cruz-Ramírez A, Hernández-Hernández E, Miranda-Pérez

- A, et al. Simulation on the effect of porosity in the elastic modulus of SiC particle reinforced Al matrix composites. *Metals*. 2020;10(3):391. <http://doi.org/10.3390/met10030391>.
32. CEA. Cast3M: Finite element modeling software [Internet]. 2024 [cited 2024 Sept 13]. Available from: <http://www-cast3m.cea.fr/>.
33. Mansouri K, Chermime B, Saoudi A, Djebaili H, Litim A, Kabouche Z. Effect of reinforcing particle shape on the behavior of composites materials. *J Nano Electron Phys*. 2021;13(6):06018. [http://doi.org/10.21272/jnep.13\(6\).06018](http://doi.org/10.21272/jnep.13(6).06018).
34. Huang H, Talreja R. Effects of void geometry on elastic properties of unidirectional fiber reinforced composites. *Compos Sci Technol*. 2005;65(13):1964-81. <http://doi.org/10.1016/j.compscitech.2005.02.019>.
35. Gorbounov M, Taylor J, Petrovic B, Masoudi Soltani S. A technical review on & roadmap for optimization of carbonaceous adsorbents and adsorption processes. *S Afr J Chem Eng*. 2022;41(1):111-28. <http://doi.org/10.1016/j.sajce.2022.06.001>.
36. Touati S, Ghelani L, Zemmouri A, Boumediri H. Optimization of gas carburizing treatment parameters of low carbon steel using Taguchi and grey relational analysis (TA-GRA). *Int J Adv Manuf Technol*. 2022;120(11):7937-49. <http://doi.org/10.1007/s00170-022-09302-0>.
37. Pino GGD, Bezazi A, Boumediri H, Kieling AC, Garcia SD, Torres AR, et al. Optimal tensile properties of biocomposites made of treated Amazonian curauá fibers using Taguchi method. *Mater Res*. 2021;24(Suppl 2):e20210326. <http://doi.org/10.1590/1980-5373-mr-2021-0326>.
38. Laouissi A, Blaoui MM, Abderazek H, Nouioua M, Bouchoucha A. Heat treatment process study and ANN-GA based multi-response optimization of c45 steel mechanical properties. *Met Mater Int*. 2022;28(12):3087-105. <http://doi.org/10.1007/s12540-022-01197-6>.
39. Telli S, Ghodbane H, Laouissi A, Zamouche M, Kadmi Y. Remediation of cationic dye from wastewater using a new environmentally friendly adsorbent: a response surface methodology and artificial neural network modeling study. *Int J Chem Kinet*. 2025;57(1):16-39. <http://doi.org/10.1002/kin.21756>.
40. Del Pino GG, Bezazi A, Boumediri H, Valin Rivera JL, Kieling AC, Garcia SD, et al. Numerical and experimental analyses of hybrid composites made from amazonian natural fibers. *Journal of Research Updates in Polymer Science*. 2023;12:10-8. <http://doi.org/10.6000/1929-5995.2023.12.02>.
41. Benkhelladi A, Laouissi A, Laouici H, Bouchoucha A, Karmi Y, Chetbani Y. Assessment of hybrid composite drilling and prediction of cutting parameters by ANFIS and deep neural network approach. *Int J Adv Manuf Technol*. 2024;135(1-2):1-18. <http://doi.org/10.1007/s00170-024-14513-8>.